Environmental Pollution 207 (2015) 31–42

Contents lists available at ScienceDirect

Environmental Pollution

journal homepage: www.elsevier.com/locate/envpol

Source contributions and regional transport of primary particulate matter in China

Jianlin Hu [a], Li Wu [b], Bo Zheng [c], Qiang Zhang [d], Kebin He [c], Qing Chang [e], Xinghua Li [e], Fumo Yang [f], Qi Ying [b], Hongliang Zhang [g, *]

[a] Jiangsu Key Laboratory of Atmospheric Environment Monitoring and Pollution Control, Jiangsu Engineering Technology Research Center of Environmental Cleaning Materials, Collaborative Innovation Center of Atmospheric Environment and Equipment Technology, School of Environmental Science and Engineering, Nanjing University of Information Science & Technology, 219 Ningliu Road, Nanjing, 210044, China
[b] Zachry Department of Civil Engineering, Texas A&M University, College Station, TX, 77843-3136, USA
[c] State Key Joint Laboratory of Environment Simulation and Pollution Control, School of Environment, Tsinghua University, Beijing, 100084, China
[d] Ministry of Education Key Laboratory for Earth System Modeling, Center for Earth System Science, Tsinghua University, Beijing, 100084, China
[e] School of Chemistry & Environment, Beihang University, Beijing, 100191, China
[f] Key Laboratory of Reservoir Aquatic Environment, Chongqing Institute of Green and Intelligent Technology, Chinese Academy of Sciences, Chongqing, 400714, China
[g] Department of Civil and Environmental Engineering, Louisiana State University, Baton Rouge, LA, 70803, USA

ARTICLE INFO

Article history:
Received 21 April 2015
Received in revised form
16 July 2015
Accepted 21 August 2015
Available online 1 September 2015

Keywords:
Primary particulate matter
Source apportionment
Regional transport
China

ABSTRACT

A source-oriented CMAQ was applied to determine source sector/region contributions to primary particulate matter (PPM) in China. Four months were simulated with emissions grouped to eight regions and six sectors. Predicted elemental carbon (EC), primary organic carbon (POC), and PPM concentrations and source contributions agree with measurements and have significant spatiotemporal variations. Residential is a major contributor to spring/winter EC (50–80%), POC (60%–90%), and PPM (30–70%). For summer/fall, industrial contributes 30–50% for EC/POC and 40–60% for PPM. Transportation is more important for EC (20–30%) than POC/PPM (<5%). Open burning is important in summer/fall of Guangzhou and Chongqing. Dust contributes to 1/3–1/2 in spring/fall of Beijing, Xi'an and Chongqing. Based on sector–region combination, local residential/transportation and residential/industrial from Heibei are major contributors to spring PPM in Beijing. In summer/fall, local industrial is the largest. In winter, residential/industrial from local and Hebei account for >90% in Beijing.

1. Introduction

Airborne particulate matter (PM) has adverse effects on visibility, climate and ecosystems in addition to human health (Cao et al., 2012; Menon et al., 2008; Poschl, 2005; Pui et al., 2014). Fine particle with aerodynamic diameter of 2.5 μm or less ($PM_{2.5}$), is especially harmful because it can penetrate deep into lungs and bloodstream. $PM_{2.5}$ has various components, which can be categorized as primary PM (PPM) because they are directly emitted and secondary PM because they are secondarily formed through chemical and physical atmospheric processes. The chemical composition of $PM_{2.5}$ is complex and is typically composed of elemental carbon (EC), primary organic carbon (POC), metals and trace elements, sulfate, nitrate, ammonium, and secondary organic aerosols (SOA). The physical and chemical formation, transformation and fate of particles are different due to their sources, morphologies, chemical compositions, and mechanical/optical properties (Kleeman and Cass, 2001; Zhang et al., 2014b, 2008).

In the past few decades, developing countries such as China and India have been facing extreme PM pollution problems due to the combination of fast increase of population, industrialization, urbanization and associated energy consumption and lagging of sufficient emission control measures (Chan and Yao, 2008; Hu et al., 2014a; Wang et al., 2014b). However, air pollution control has significant economic cost associated with it due to reduction of economic activities, migration and upgrade of industries, and modernization of energy infrastructures, etc. Thus, it is important to prioritize the emission control targets and determine the cost-effective emission reductions.

* Corresponding author.
E-mail address: hlzhang@lsu.edu (H. Zhang).

http://dx.doi.org/10.1016/j.envpol.2015.08.037
0269-7491/

Contributions of different source sectors and regions are the critical information needed for policy makers to design effective emission control strategies. Receptor-oriented techniques have been applied at different regions of China to obtain such information (Tao et al., 2014; Zhang et al., 2013). These receptor-oriented statistical source apportionment methods are highly observation dependent and in need of a large amount of observations with detailed components information, which is not available for most regions where only PM mass concentration measurements are available. State-of-art measurement equipment such as aerosol mass spectrometry (AMS) and aerosol chemical speciation monitor (ACSM) greatly increased the abundance of observation samples in China (He et al., 2011; Sun et al., 2014). Such techniques based on more detailed organic aerosol measurements lead to improved understanding of the sources of PM but they can only resolve contributions to OA and are also limited to only provide local source attribution information at the observation site.

Chemical transport model (CTM) based techniques have also been applied to investigate sources to $PM_{2.5}$ (Kleeman et al., 2007; Ying et al., 2008; Zhang et al., 2014b), but only a few studies have been conducted in China. For example, CMAQ with the brute force method (BFM) was used by Wang et al. (2013) to identify the contributions of both source regions and sectors to $PM_{2.5}$ in Southern Hebei during the 2013 severe haze episode. Decoupled direct method (DDM) as an imbedded sensitivity tool in some CTMs has also been used to determine the importance of different sources (Cohan et al., 2005; Dunker et al., 2002). However, both the BFM and the DDM method are more suitable to estimate the change of PM concentrations due to proposed emission control measures than to determine the contributions of certain sources because removal of PM emissions could affect the transport, chemistry, deposition and interactions with meteorology although they are not chemically reactive (Zhang and Ying, 2011). In addition, the BFM method needs to repeat CTM simulations multiple times and greatly increases the computational cost.

Since primary and secondary $PM_{2.5}$ are formed through different formation pathways and have different chemical composition and regional transport characteristics, it is essential to design source apportionment studies to focus on different PM components separately. Contributions of different source sectors and regions to sulfate and nitrate concentrations in January and August 2009 in China were quantified using a reactive tracer based source apportionment technique (Ying et al., 2014; Zhang et al., 2012). These two studies showed the importance of secondary inorganic components in total $PM_{2.5}$ concentrations. Power sector, transportation, and industrial activities were the dominating source of nitrate and sulfate in both January and August while residential sector contributed to approximately 10–20% of nitrate and sulfate in January. Significant inter-regional transport of nitrate and sulfate was also predicted. However, source and source region contributions to PPM have not been studied in these studies. In addition, the emission inventory used in these studies is for year 2006 and the results cannot be used to interpolate extremely high $PM_{2.5}$ concentrations in recent years. Wang et al. (2014a) quantified the source contributions to both primary and secondary inorganic PM in Xi'an, a major metropolitan in Northwest China and showed that majority of $PM_{2.5}$ was from energy generation (5%), industries (58%) and residential activities (16%) during an extremely polluted month in winter 2013. This study only focused on a small region and a specific month, source contributions to primary and total $PM_{2.5}$ in other areas and the seasonal variations are still not clear.

In this study, a source-oriented air quality model is developed to quantify the contributions of different source sectors and regions to PPM mass as well as its major components EC and POC. The model was applied in a four-month study during 2012–2013 in China to compare the seasonal variations in the region- and source-contributions to PPM. The model results provide valuable information for policy makers to design feasible control measures that balance air pollution reduction and economic costs.

2. Method

2.1. Model description

An updated source-oriented CMAQ model for PPM (CMAQ-PPM) based on CMAQ v5.0.1 (SAPRC-07 photochemical mechanism and AERO6 aerosol module) was developed to determine the source sector and source region contributions to PPM. In the CMAQ-PPM model, tagged non-reactive PM tracers that bear the source sector and region information are used to determine the regional distribution of PPM and its chemical components from multiple emission source sectors and regions in a single model simulation. For example, a tracer ATCR1_2J is used to represent the accumulation mode PPM from source type 1 and source region 2. In this version of the CMAQ-PPM model, emissions from 8 source regions and 9 source types can be tracked simultaneously. These PM tracers are treated as inert PM chemical components and go through the same advection, diffusion, coagulation and deposition processes as other PM components, such as the trace metals in AERO6. As the tracers are considered as non-reactive, no changes to the gas phase chemical mechanism and aerosol chemistry are necessary. In each grid cell, the emission rates of the tracers are set to be a very small fraction (1×10^{-5}) of the PPM emission rates from the corresponding source sectors and regions to make sure that they will not significantly change the particle mass and size distribution to affect other physical and chemical processes. For example, if a grid cell resides in source region 2 and the PPM emission rate of source type 1 in that grid cell is 1 g s^{-1}, the emission rate of the non-reactive PM tracer ATCR1_2J will be set to 1×10^{-5} g s^{-1}. The predicted tracer concentration in a given grid cell, after scaling up by 1×10^5, represents total primary $PM_{2.5}$ mass concentration from a specific source type/region combination in that grid cell. The concentrations of the inert chemical components in primary $PM_{2.5}$ can be determined during the post-processing stage using source specific emission profiles, as shown in equation (1):

$$C_{i,j} = A_{i,j} T_i \quad (1)$$

where $C_{i,j}$ represents the concentration of the jth chemical component from the ith particle emission source category. A is the source profile matrix so that $A_{i,j}$ represents the mass of the jth chemical species per unit mass of PM emitted from the ith emission source. T_i is the model predicted particle mass concentration for the ith source based on the source specific tracer concentrations, as described above. Fig. S1 shows maximum less than 10% difference between the predicted POC and EC in October 2012 by the original CMAQ and CMAQ-PPM models, confirming that the model results were not significantly affected by this technique. Although 72 tracers (9 source regions × 8 source types) are added to the model, the computational time is only slightly increased by less than 10% of the original CMAQ model.

Unlike previous versions of the source-oriented PPM source apportionment models using similar tagging techniques that disabled chemistry and secondary PM formation to reduce run time (Hu et al., 2014b; Wang et al., 2014a), the CMAQ-PPM used in this study includes a full description of the gas and aqueous phase chemistry and gas-to-particle partitioning processes. This is necessary for areas with very high PM concentrations and a significant fraction of secondary PM, as neglecting secondary PM leads to significant biases in the predicted primary particle size and mass concentrations.

Emissions of PPM from windblown dust and sea salt are calculated inline. The original inline dust module in CMAQ depends on the USGS land use information used in the inline biogenic emission module. It was modified to work with the 20-category MODIS land use data in this study. Equation to estimate the vertical dust flux was modified to follow that of Shaw et al. (2008) and the PM_{10} fraction in total PM emission is estimated based on Choi and Fernando (2008). The same equations were used in an offline dust module in previous applications of CMAQ in China (Ying et al., 2014; Zhang et al., 2012). Photolysis rates are also calculated inline to correctly account for the reduction of actinic flux due to high aerosol loading.

2.2. Model application

The CMAQ-PPM model was applied to study the source sector and region contributions to PPM in China using a 36-km horizontal resolution domain. There are 18 stretching vertical layers in the CMAQ domain, with a first layer thickness of approximately 35 m. Four 1-month episodes in 2012 (August and October) and 2013 (January and March) were simulated, which represent summer, fall, winter and spring, respectively. The meteorological inputs were generated using the Weather Research and Forecasting (WRF) model version 3.6 with initial and boundary conditions from the NCEP FNL Operational Model Global Tropospheric Analyses dataset. There are 29 vertical layers in the WRF simulation. The first 8 layers of the WRF and CMAQ domains are identical. Detailed WRF model configurations have been described by Zhang et al. (2012).

Anthropogenic emissions were generated based on the Multi-resolution Emission Inventory for China (MEIC) developed by Tsinghua University (http://www.meicmodel.org). Compared with previous inventories such as TRACE-P (Streets et al., 2003) or INTEX-B (Zhang et al., 2009), the major improvements of MEIC include a unit-based emission inventory for power plants (Wang et al., 2012b), cement plants (Lei et al., 2011), high-resolution county-level vehicle emission inventory (Zheng et al., 2014), and a novel NMVOC mapping approach for different chemical mechanisms (Li et al., 2014). VOC emissions have already been speciated for the SAPRC-07 mechanism. $PM_{2.5}$ emissions were speciated into AERO6 model species using profiles adapted from the SPECIATE database. As emissions of EC and OC were also provided directly by MEIC, they were not generated using source profiles from $PM_{2.5}$ emissions. The speciation profiles were renormalized to ensure that the sum of the components were equal to the total PPM emissions. Emissions from other countries and regions outside China were generated using the gridded 0.25 × 0.25 resolution Regional emission inventory in ASia version 2 (REAS2) (Kurokawa et al., 2013).

Biogenic emissions were generated using the Model for Emissions of Gases and Aerosols from Nature (MEGAN) v2.1. The leaf area index (LAI) were based on the 8-day Moderate Resolution Imaging Spectroradiometer (MODIS) LAI product (MOD15A2). The plant function types (PFTs) were based on the PFT files used in the Global Community Land Model (CLM 3.0). Open biomass burning emissions were generated from the Fire INventory from NCAR (FINN), which is based on satellite observations (Wiedinmyer et al., 2011). Dust and sea salt emissions were generated during the CMAQ simulations, as described in the previous section.

PPM mass emissions were grouped into eight regions and cities in China: (1) Beijing, (2) Hebei, (3) Northeast, (4) Northwest, (5) Central, (6) Southeast, (7) Southwest, and (8) Shanghai (see Fig. 1), were tracked separately in this study. Furthermore, emissions within each region were grouped into four anthropogenic sectors: (1) residential, (2) transportation, (3) power, and (4) industrial. Open burning emissions are considered as the 5th emission sector. Total PPM emissions from windblown dust due to soil erosion were also treated as separate emission sector although the source origins were not tracked.

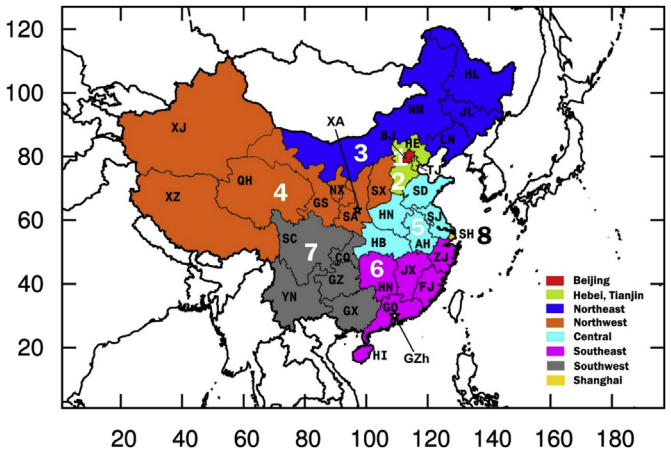

Fig. 1. Model domain and designation of source regions. Axes are the number of grid cells. Locations of the five selected cities are also shown (BJ Beijing, SH Shanghai, GZh Guangzhou, XA Xi'an, and CQ Chongqing).

3. Results

3.1. Meteorology and air quality validation

Meteorology plays an important role in air pollution formation (Zhang et al., 2015). The predicted temperature (T2) and relative humidity (RH) at 2 m above surface, and wind speed (WS) and wind direction (WD) at 10 m above surface are compared with observation data from the National Climatic Data Center (NCDC). There are ~1200 stations within the domain with hourly or every-third-hour observations. The observations from the stations are compared with the WRF predictions at the grid cells where the stations are located. Model performance statistics including mean observation (OBS), mean prediction (PRE), mean bias (MB) and gross error (GE) are calculated and the results are shown in Table 1. Generally WRF model has good performance on the meteorological conditions and the performance statistics are comparable to other studies using WRF (Dzepina et al., 2009; Fast et al., 2006; Misenis and Zhang, 2010; Zhang et al., 2014a).

Table 1
Meteorology performance over the whole domain in the four months (OBS, observation; PRE, prediction; MB, mean bias; and GE, gross error).

Variable	Statistics	Jan. 2013	Mar. 2013	Aug. 2012	Oct. 2012
T2 (K)	OBS	268.4	277.5	297.0	285.2
	PRE	367.4	276.2	296.1	285.4
	MB	−1.0	−1.3	−0.9	0.2
	GE	3.5	3.0	2.7	2.8
WS (m/s)	OBS	3.4	3.7	3.3	3.4
	PRE	4.7	4.8	4.2	4.4
	MB	1.3	1.1	0.9	1.0
	GE	1.9	1.9	1.8	1.8
WD (degree)	OBS	211.1	205.0	171.7	193.2
	PRE	231.3	220.4	169.8	198.2
	MB	20.2	15.4	−1.9	5.0
	GE	49.0	46.7	54.8	51.9
RH (%)	OBS	76.6	69.5	69.1	68.9
	PRE	69.8	68.4	71.0	67.2
	MB	−6.8	−1.1	−1.9	−1.7
	GE	15.6	15.4	14.1	14.6

Table 2
Fractions of EC and OC in PPM emissions for the source sectors tracked in this study (%).

Source sector	EC fraction	OC fraction	Source
Residential	0.201	0.563	MEIC domain average
Transportation	0.559	0.202	MEIC domain average
Power	0.002	0.001	MEIC domain average
Industrial	0.104	0.103	MEIC domain average
Open burning	0.095	0.556	SPECIATE 4.3 (92090)
Dust	0.002	0.031	SPECIATE 4.3 (92001)

$PM_{2.5}$ mass and component concentrations used to evaluate the model performance were measured during the 2012–2013 period on Beihang University (BUAA) campus (Wang et al., in press), which is located near the north forth ring in Beijing and about 12 km northwest of the city center. Daily 23-hr integrated (1 h was left each day for changing filters) $PM_{2.5}$ samples were collected using a five-channel Spiral Ambient Speciation Sampler (SASS, Met One Inc.). Two 47 mm Teflon filters were used to collect $PM_{2.5}$ for mass and elements, and water soluble ions analysis, respectively. A quartz fiber filter was used to collect $PM_{2.5}$ for EC and OC analysis. In addition, EC concentrations during a one-week episode in January 2013 in Beijing, Shanghai, and Guangzhou reported in a recent study (Andersson et al., 2015) were also used in evaluating the model performance. Fractions of EC and OC in PPM emissions from the sources tracked in this study are shown in Table 2. They were used to determine source sector and region contributions to EC and OC in the following analyses.

Fig. 2a compares the observed and predicted EC concentrations at BUAA in Beijing during the four seasons. General agreement is found between the predictions and observations, with more than 80% of data points falling into the 1:2 and 2:1 lines. EC concentrations are higher in winter and spring and lower in fall and summer. The mean fractional biases (MFBs) of EC are −0.24, 0.08, −0.06, and 0.05 in the spring, summer, fall, and winter, respectively. Fig. 2b compares the observed and predicted EC in Beijing, Shanghai, and Guangzhou during the 1-week sampling episode in January, 2013 based on data from Andersson et al. (2015). The results show good agreement at Guangzhou for 7 days, at Shanghai for 5 days, and at Beijing for 4 days. On 2–3 days at Beijing and Shanghai, the discrepancy between model predictions and observations is significant. The uncertainties of meteorology and emissions could be reasons of those data out of 1:2 and 2:1 lines. For example, weekly and diurnal profiles were used to calculate hourly emission rates, which would miss the special circumstances. The model performance on EC in the whole January shown in Fig. 2a suggests that the model successfully reproduced the monthly average EC concentrations. In addition, the good agreement with observations on most of the days at the three sites located in widely different regions builds confidence in the model results in other regions where no observations are available.

Fig. 2c shows the predicted and estimated POC based on measured total OC. Previous studies have utilized OC/EC ratio to determine POC fractions in OC, so this method was adopted in the present study to estimate the daily observed POC concentrations using equation (2):

$$POC = EC \times (OC/EC)_{min} \quad (2)$$

where $(OC/EC)_{min}$ is the minimum of the OC/EC ratios (Castro et al., 1999). The $(OC/EC)_{min}$ values are 2.21, 1.45, 1.25, and 2.08 for spring, summer, fall, and winter, respectively. The daily POC/OC ratios range 39–98% in the spring, 38–85% in summer, 11–64% in fall, and 36–100% in winter, respectively. The ranges are generally consistent with previous studies in Beijing (Alexander et al., 2009; Guo et al., 2012; Lin et al., 2009; Sun et al., 2014; Zhao et al., 2013). Predicted POC is generally in good agreement with the estimated POC concentrations, with MFBs of −0.30, 0.13, 0.18 and 0.17 in spring, summer, fall, and winter, respectively.

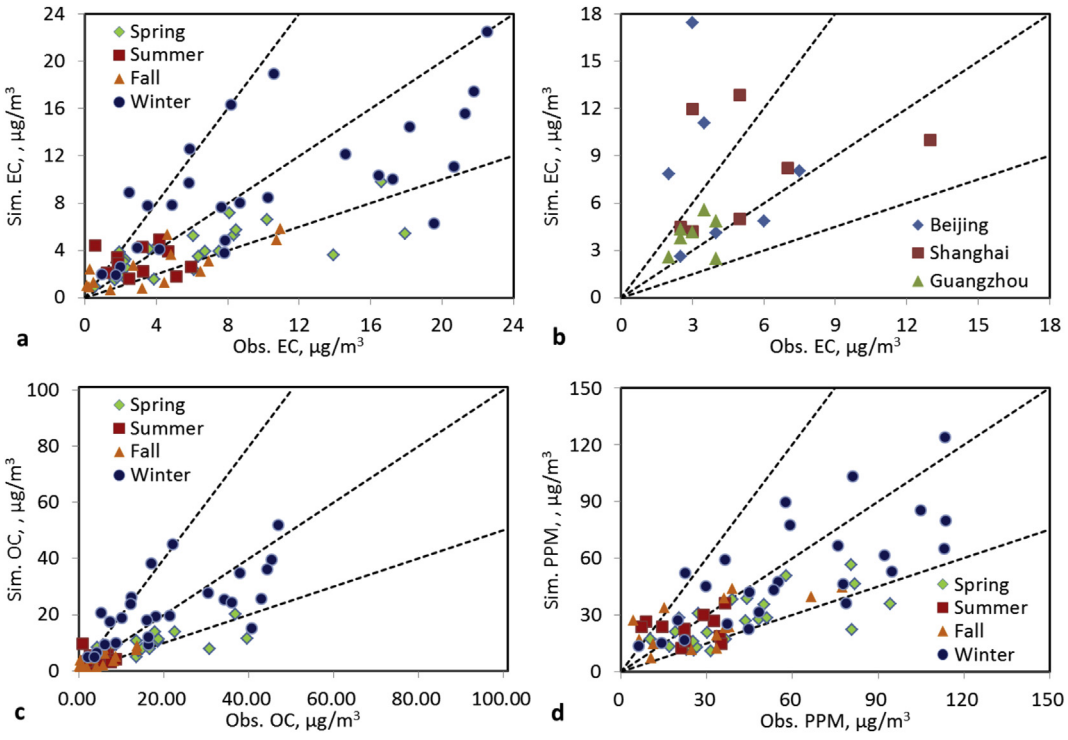

Fig. 2. Observed and model simulated EC, POC, and PPM concentrations.

Fig. 2d show the predicted PPM vs. the estimated PPM based on measured concentrations. Fig. S2 also shows the time series of predicted PPM and observations in Beijing as well as source sector based apportionment results. The estimated PPM was calculated by deducting sulfate, nitrate, ammonium, and estimated secondary organic matter (OM). It should be noted that some of the sulfate might be primary sulfate from coal-fired power plants. However, the low contributions of power plant emissions to PPM and generally large concentrations of total sulfate implies that primary sulfate will only account for a small fraction (less than 5%) of total sulfate (Zhang et al., 2012). Thus, the impact of excluding the primary sulfate on the estimated PPM is small. 83% of data points fall into the 1:2 and 2:1 lines. Good agreement is found between the predicted and estimated PPM concentrations higher than 20 $\mu g/m^3$ except for a few data points in spring, when over-prediction occurs for low observed values. The overall MFBs are −0.39, 0.01, −0.07, and −0.09 for spring, summer, fall, and winter, respectively.

As an additional evaluation of the model capability in reproducing observed PM concentrations, the model performance of total $PM_{2.5}$ in 59 major cities in March 2013 is shown in Table S1. MFB and MFE values show that the model generally reproduce the total $PM_{2.5}$ observations in 53 cities (~90%), with the MFB and MFE meeting the model performance criteria (MFE≤+75% and MFB≤±60%) suggested by Boylan and Russell (2006). Model predictions of total $PM_{2.5}$ concentrations generally agree with observations in the cities located in the North China Plain (NCP), the Yangtze River Delta (YRD), and the Pearl River Delta (PRD), which are the most populated and also heavily polluted regions in China.

3.2. Source apportionment of PPM

Fig. 3 shows the comparison of the relative source contributions to $PM_{2.5}$ EC from combustion sources during 2013 January at three sites of Beijing, Shanghai, and Guangzhou estimated by a dual carbon isotope constrained (Δ14C and Δ13C) source apportionment study (Andersson et al., 2015), and by the source-oriented CMAQ-PPM model in the present study. The source categories constrained by the carbon isotopes are biomass burning, liquid fossil fuel combustion, and coal combustion. To get consistent sources from the CMAQ results, sources in the present study e.g., power, industry, residential, transportation, and open burning were further broken down into the three categories according to the energy consumption data provided by Wang et al. (2012a). Detailed fractions are listed in Table 3. Fig. 3 indicates the source contributions estimated by the two methods are consistent at the three sites, especially when the 95% confidence interval in the carbon isotope method was considered. The general agreement in the two source apportionment studies at three different sites further builds confidence for using the source apportionment results of this study in other locations and seasons.

The CMAQ-PPM results were also examined by comparing to the results with four BFM simulations: a) zeroing out all residential emission, b) zeroing out all industry emission, c) zeroing out residential emission in Beijing, and d) zeroing out all transportation emission in Hebei. Differences between the base case and the emission-zero-out cases are considered as the source contributions identified by BFM and were compared with CMAQ-PPM results. Fig. S3 shows the comparison of contributions of residential and industry to EC and POC predicted by CMAQ-PPM and BFM in October 2012 in five cities, and Fig. S4 compares the contributions of residential emissions emitted in Beijing and transportation emission emitted from Heibei to EC and POC concentrations in Beijing. Generally the two methods yield similar results. Some differences are found in the results estimated by the two methods, especially for EC from residential in Shanghai and Guangzhou. The

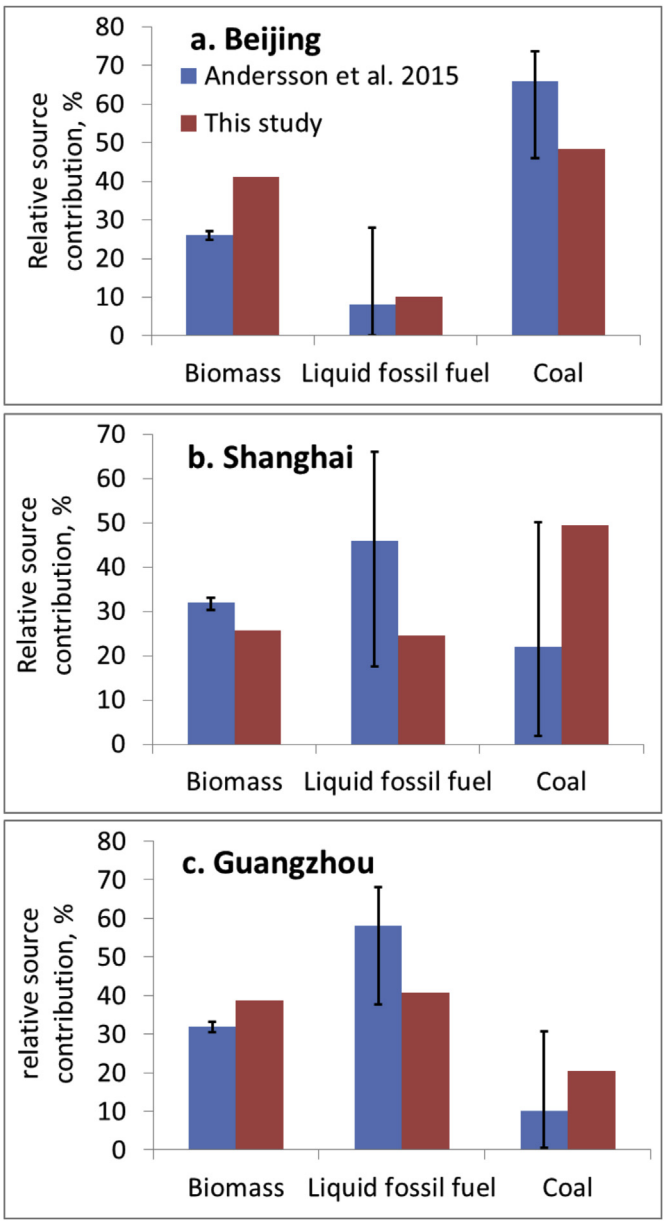

Fig. 3. Comparison of source contributions to EC from this study with another study at Beijing, Shanghai and Guangzhou (Andersson et al., 2015).

differences are likely caused by 1) the domain-average source profiles used in the CMAQ-PPM to determine component concentrations and 2) differences in the predicted removal of PPM and its chemical components in the BFM simulations due to reduction of PPM emissions that alters the particle size.

Fig. 4 shows the seasonal variations in the source contributions to EC in five megacities: Beijing, Shanghai, Guangzhou, Xi'an, and Chongqing. These five megacities have high population density and contribute to more than 15% of total population in China. They are also good representatives of different pollution patterns in different regions of China (Hu et al., submitted for publication). EC concentrations in all the five cities exhibit similar seasonal pattern, with the lowest concentrations of 2~3 $\mu g/m^3$ in the summer, and the highest in the winter. Locations of the five cities can be found on Fig. 1. The winter concentrations are 3~4 times greater than summer in all the cities, except Guangzhou. Beijing, Xi'an, and

Table 3
Factors of source sectors to fuel categories.

	Beijing			Shanghai			Guangzhou		
	Biomass	Liquid fossil fuel	Coal	Biomass	Liquid fossil fuel	Coal	Biomass	Liquid fossil fuel	Coal
Residential	0.532	0.002	0.466	0.491	0.006	0.503	0.869	0.019	0.112
Traffic	0.000	1.000	0.000	0.000	1.000	0.000	0.000	1.000	0.000
Power	0.000	0.000	1.000	0.000	0.001	0.999	0.000	0.007	0.993
Industrial	0.000	0.071	0.929	0.000	0.197	0.803	0.000	0.479	0.521

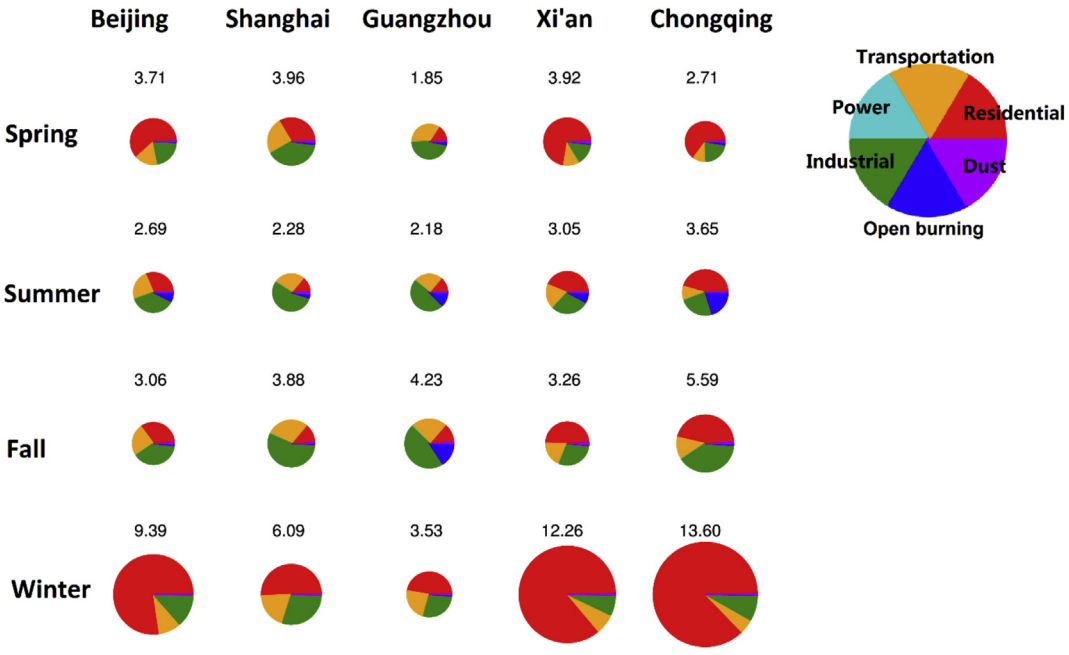

Fig. 4. Seasonal variations in the source contributions to EC. Units are μg/m^3.

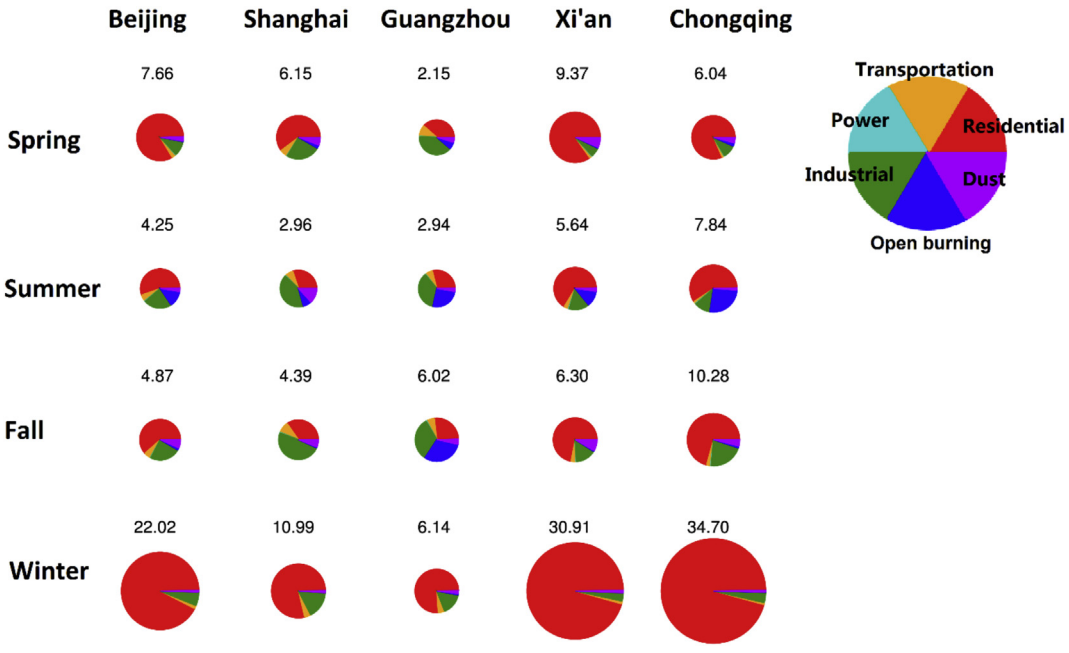

Fig. 5. Same as Fig. 4, but for POC.

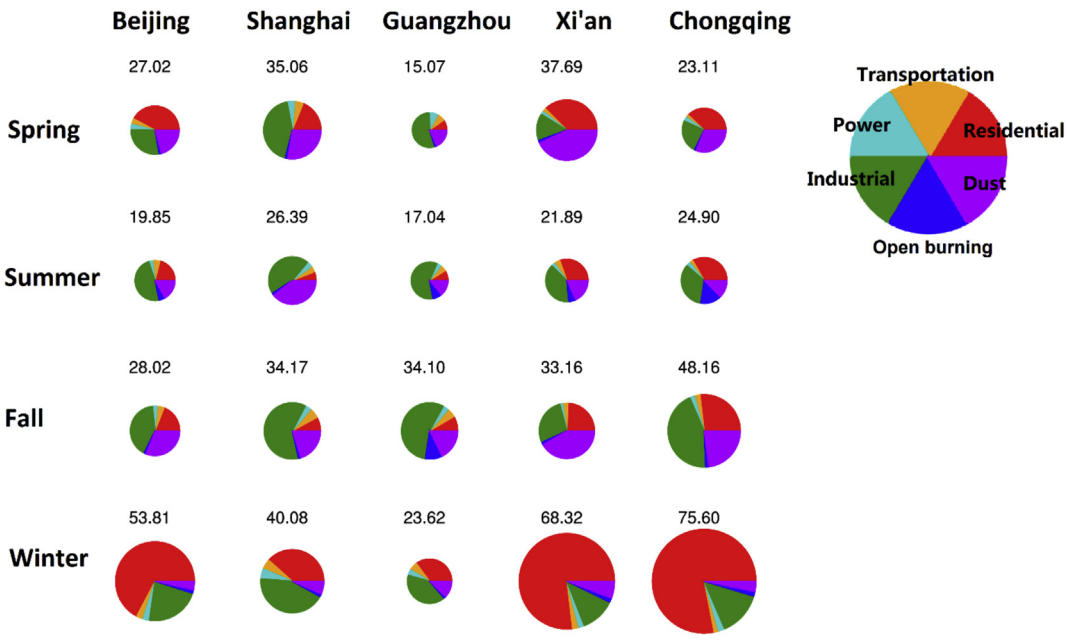

Fig. 6. Same as Fig. 4, but for PPM.

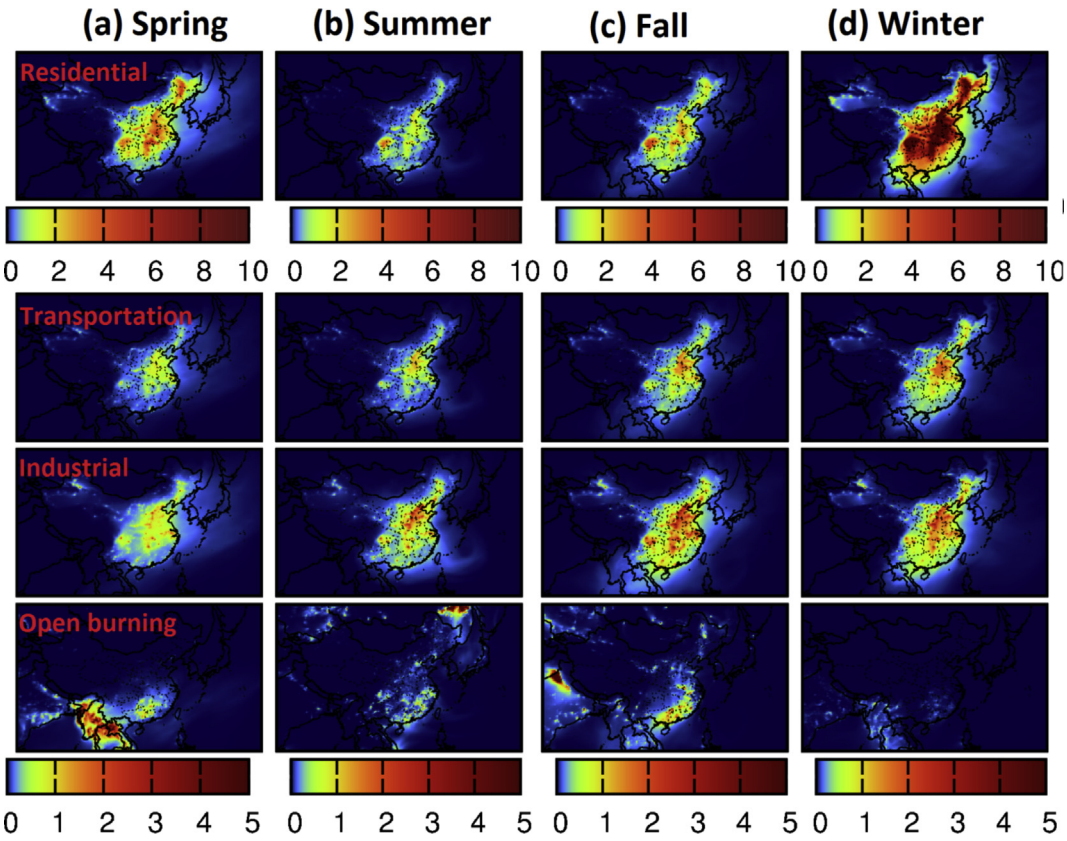

Fig. 7. Regional source apportionment of EC in the four seasons. Units are μg/m^3.

Chongqing have similar EC sources, with the residential sector as the dominant source almost in all seasons, especially in the cold winter and spring seasons. In summer and fall, the contribution from industrial sector becomes more significant. In Shanghai and Guangzhou, the residential sector is still the dominant source in the winter, but industrial sector contributes more in the all other three seasons. Transportation is the 3rd largest source to EC overall, and contributes 20–40% in Guangzhou. Power plants have insignificant contribution to EC in all the cities. Open burning has some contributions in summer and fall, but could become an important source

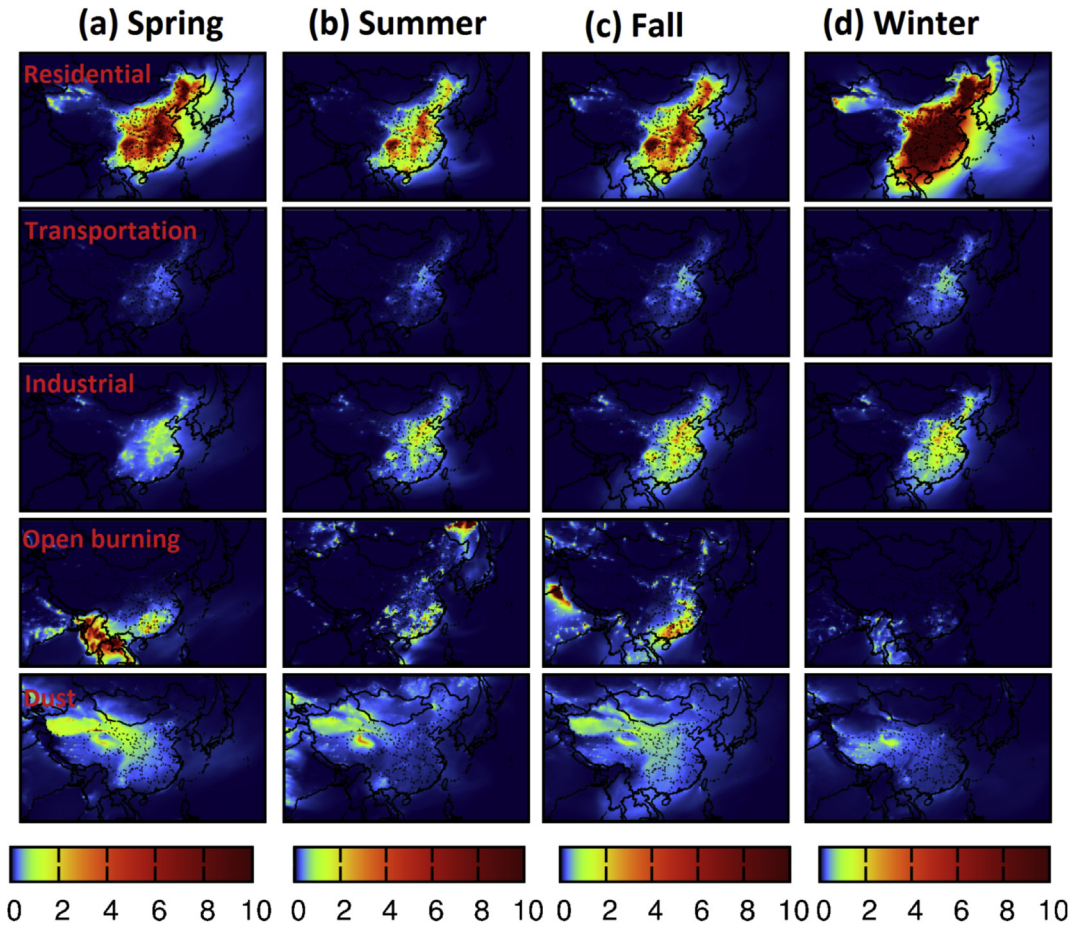

Fig. 8. Same as Fig. 7, but for POC.

in the summer for Chongqing and in the fall for Guangzhou.

Fig. 5 shows the sources of POC in the five megacities and seasonal variations in their contributions. Residential sector again is the largest source for POC in all cities overall, followed by industrial sector. Similar to the trend in EC contribution, the contribution of residential sources is greater in the winter and the spring, while the contribution of industrial sources accounts for more fractions in the summer and the fall. Different from the source contribution in EC, transportation becomes less important to POC, while open burning could be an important source of POC in the summer and the fall of Guangzhou and in the summer of Chongqing, accounting for over 30% of total POC concentrations.

Fig. 6 shows the sources of total PPM in the five megacities and seasonal variations in their contributions. Residential, industrial, and dust are the three major source sectors in all the cities, with combined contributions of 90% or more in most seasons. Residential sources dominate the PPM concentrations in winter in Beijing, Xi'an, and Chongqing, while industrial sources dominate in summer. Dust contributes nearly half of the PPM in Xi'an in spring and fall, and 1/4 to 1/3 in Beijing and Chongqing in spring and in fall. Industrial sources are the most important sources of PPM in Shanghai and Guangzhou, especially in the fall season, which could contribute to over 60% of the PPM concentrations.

Fig. 7 shows the predicted source contributions to EC in the four seasons. Power and dust are not shown due to their minor contributions. EC from the residential sector shows clear seasonal and spatial trends. Residential sources are mainly in eastern China, with high concentrations in the NCP, Sichuan Basin, and the Northeast Plain. The sources are widely distributed in these regions, affecting large areas and population in these regions. The contribution of residential sector to EC can be > 10 $\mu g/m^3$ in winter in most populated areas. Its contribution is much less in summer, but still can be > 4 $\mu g/m^3$ in the Sichuan Basin. Industrial sector has a similar spatial pattern as the residential sector, but shows smaller seasonal variations. The contributions of industrial sector are up to 5 $\mu g/m^3$ in the NCP in summer, fall, and winter, and slightly lower in spring. Contribution of transportation is mainly in the NCP and YRD in spring and summer. Unlike residential and industrial sources, contributions of transportation in other regions are generally low. Open burning sector shows very strong seasonal and spatial variations. In China, open burning, mainly intensive agriculture waste burning, occurs in the southern China in spring and fall, and more open burning in summer scatters across southern China, the YRD, and the Sichuan Basin. Open burning in Southeast Asia countries in spring (agriculture waste burning) and in Russia in summer (forest fire) could also affect the EC concentrations in the provinces near the sources.

Fig. 8 shows the source types contributing to POC in the four seasons. The general spatial pattern and seasonal variation of POC contributions from the residential, transportation, industrial, and open burning sources are similar to those of EC. Residential is the single dominant source for POC in China in all seasons. Industrial sector is also an important POC source in eastern China. Transportation is less important to POC, compared to its contributions to EC. Dust is not an important source of POC in northwestern China, with the maximum contribution of less than 1 $\mu g/m^3$ in spring. Fig. 9 shows the source contributions to PPM. Generally, spatial

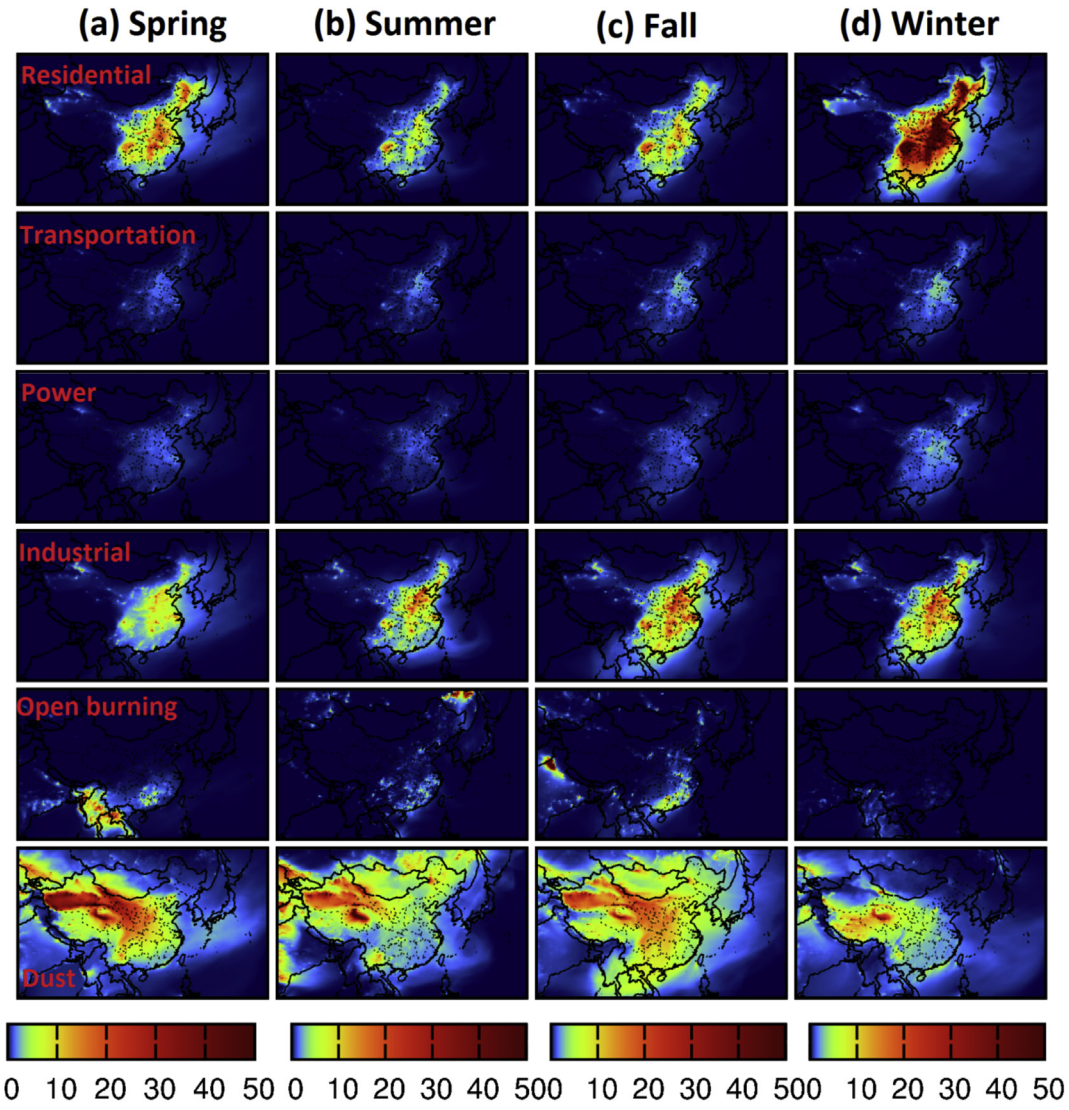

Fig. 9. Same as Fig. 7, but for PPM.

patterns of contributions from various source types to PPM are similar to those of EC and POC since they are the major components of PPM. Another important PPM component is the crustal material from windblown dust. Therefore, windblown dust becomes a more important source for PPM in China. Overall, residential, industrial, and dust are the three major sources for PPM in China in all seasons and open burning is important to PPM in southern China from spring to fall. Contributions from power and transportation sources are orders of magnitude lower.

3.3. Region-sector apportionment of PPM in Beijing

Regional transport brings emissions from different regions and mixes with the local sources. A previous study (Ying et al., 2014) has revealed that the intra- and inter-regional transport could play an important role during high secondary PM air pollution episodes in China. Fig. S5 shows that the local sources were the major sources to PPM, EC, and POC in Beijing especially in winter. Heibei, the province surrounds Beijing, could be the dominating source region in other three seasons. Contributions from other regions were small. Fig. S6 shows the results in Shanghai. Local sources were the largest contributor to PPM, EC, and OC all the seasons except for peak times when transport of emissions from central China (north and west to Shanghai) was significant. Southeast also contributed to some peaks in the spring and summer. North region and combination of Beijing and Hebei could also contribute to ~10% each at some peaks in the winter. Fig. S7 shows the contributions to PPM, EC, and OC to the Southeast, where Guangzhou is located. Local sources (Southeast) were the major contributor, but Central sources become important during high pollution events.

In particular, the region-specific source sector apportionment is useful for developing regional air pollution control strategies. Beijing was chosen to study the contributions of sources located in different regions (defined in Fig. 1) to PPM. Fig. 10 shows the predicted time series of contributions to daily averaged PPM in Beijing in the four seasons. A total of 40 region-sector sources (5 source sectors by 8 regions) were calculated and only the top 8 region-sectors are shown in Fig. 10 for better visualization purpose. All other region-sectors after the top 8 are grouped as 'other'. Majority of 'other' is due to windblown dust, especially in spring and fall. In spring, the local residential sources (Res-BJ), local transportation (Trans-BJ), residential and industrial sources from Heibei (including Tianjin) (Res-HB and Indus-HB) are the most contributors. During a peak day, they could contribute to over 40 $\mu g/m^3$ of PPM,

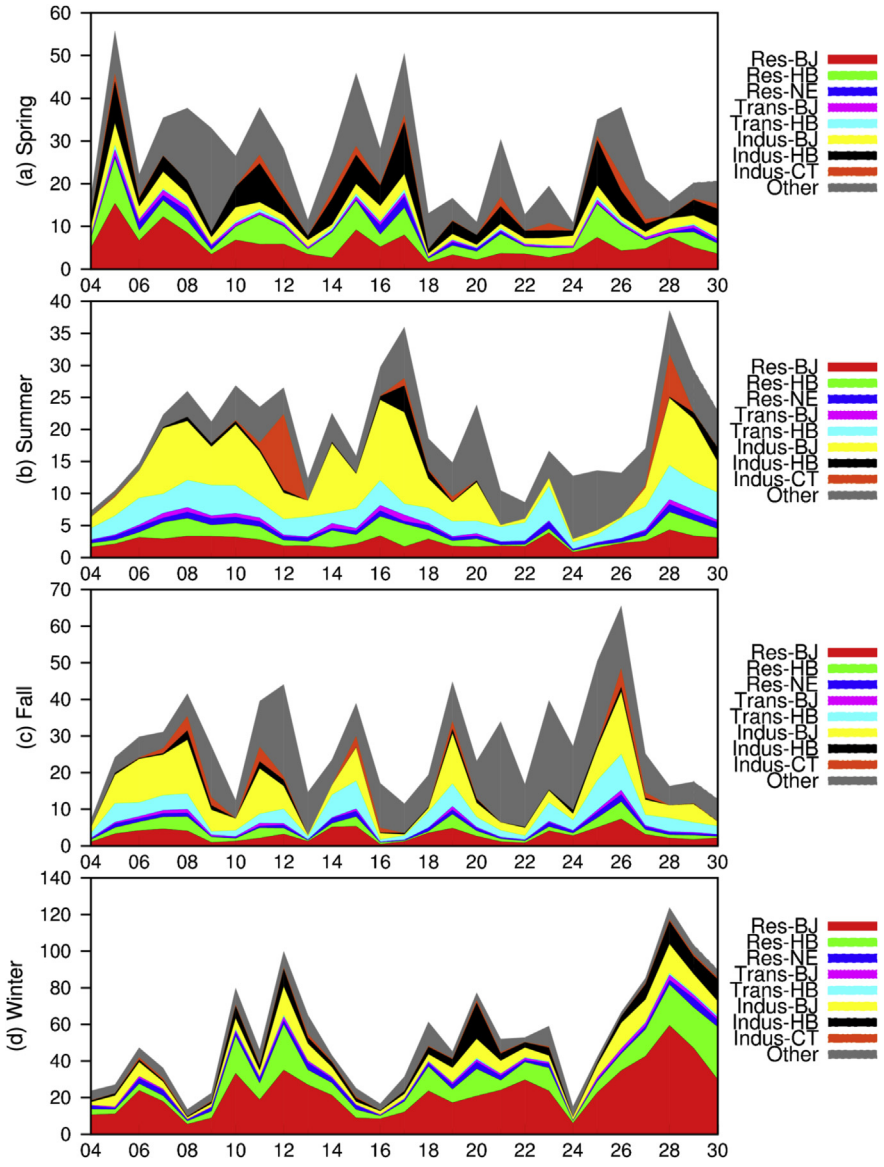

Fig. 10. Region-source contributions to daily PPM concentrations in Beijing in the four seasons. Units are $\mu g/m^3$.

accounting for 80% of the total PPM in Beijing. In the summer, the local industrial (Indus-BJ) is the largest PPM source, contributing over 15 $\mu g/m^3$ PPM during high pollution days. Local residential (Res-BJ) contributes 2–3 $\mu g/m^3$ to PPM. Transportation and residential sources from Hebei (Trans-HB and Res-HB) are important in the summer, contributing to up to 5 $\mu g/m^3$ and 3 $\mu g/m^3$ PPM in Beijing. Similar to the summer, the most important PPM region-sectors in Beijing in the fall are Indus-BH, Trans-HB, Res-BJ, and Res-HB, accounting for over 60% of the total PPM. In the winter, Res-BJ, Res-HB, Indus-BJ, and Indus-HB are the top 4 sources for PPM. The four sources could contribute >100 $\mu g/m^3$ PPM under extreme conditions, and account for >90% of the total PPM.

Fig. S8 shows the comparison of CMAQ-PPM predicted contributions to PPM, EC and POC from the transportation, power, industrial and residential sources with the emission contributions from these sources in Beijing in summer and winter, respectively. Similar contributions are identified by the two methods in winter, as the pollutants are dominant by local residential sources (Fig. S5). However, significant differences exist in the summer results. For example, power plants only accounts for 0.003% of PPM emissions in Beijing, but CMAQ-PPM predicts the contribution of power plants to PPM concentration is 4%. Residential sources contribute 37% of PPM and 50% of EC emissions, respectively, but are predicted to contribute 27% of PPM and 34% of EC concentrations, respectively. These significant differences are due to regional transport. Therefore regional transport should be considered in source apportionment studies.

4. Conclusion

In this study, a source-oriented version of the CMAQ model for PPM (CMAQ-PPM) was developed. The CMAQ-PPM uses tagged non-reactive tracers for both source sectors and regions and kept the full description of gas and aqueous chemistry and gas-to-particle partitioning. This is important in China because neglecting secondary PM for high PM concentrations could lead to biases in predicted size and mass of PPM. The model was applied to determine the source sector and region contributions to PPM in China and related spatial and seasonal variations. Good agreement of model predictions with observations of EC, estimated OC and

PPM, and winter EC source apportionment results at Beijing, Shanghai, and Guangzhou was achieved.

Significant spatial and temporal variations were observed in concentrations and source contribution of EC, POC, and PPM. Residential is the major contributor to EC (50–80%), POC (60%–90%), and PPM (30–70%) in spring/winter. Industrial is more important in summer/fall with contributions of 30–50% to EC and OC, and 40–60% to PPM. Contribution of transportation is only important for EC (20–30%) and open burning is significant for periods such as summer/fall in Guangzhou and summer in Chongqing. Dust is important in spring/fall for north and west cities, with 1/3~1/2 contributions to PPM of Beijing, Xi'an and Chongqing. To provide clear information to policy makers, the contributions of sector–region combination to PPM in Beijing was also determined. The local residential/transportation and residential/industrial from Heibei are the major contributors to PPM in Beijing during spring. In summer/fall, local industrial is the largest followed by local residential and transportation/residential from Heibei. In winter, residential/industrial emissions from local and Hebei account for >90% of PPM in Beijing.

The ability of the CMAQ-PPM model to reproduce the observed PM concentrations and source apportionment results based on other methods confirms the feasibility of air quality models to provide source apportionment information for policy making. Although the current study demonstrates the capability of the source-oriented CMAQ model associated with the 36-km resolution MEIC emission inventory to provide reasonable predictions of primary PM and its source and source region contributions, uncertainties exist especially for peak episodes due to model inputs of meteorology, accuracy of the emission inventories and model grid resolution. High spatial and temporal resolution emissions are needed to provide more accurate source apportionment results of primary PM in China.

Acknowledgment

This project is partly funded by the Startup Fund for Talent at NUIST under Grant No. 2243141501008 and the Priority Academic Program Development of Jiangsu Higher Education Institutions (PAPD), the National Natural Science Foundation of China (4127512), Jiangsu Key Laboratory of Atmospheric Environment Monitoring and Pollution Control of Nanjing University of Information Science and Technology, and Jiangsu Province Innovation Platform for Superiority Subject of Environmental Science and Engineering (No. KHK1201). LW and QY would like to thank the computation resources from the Texas A&M Supercomputing Facility (http://sc.tamu.edu/) for completing some of the model simulations reported in this study.

Appendix A. Supplementary data

Supplementary data related to this article can be found at http://dx.doi.org/10.1016/j.envpol.2015.08.037.

References

Alexander, B., Park, R.J., Jacob, D.J., Gong, S., 2009. Transition metal-catalyzed oxidation of atmospheric sulfur: global implications for the sulfur budget. J. Geophys. Res. Atmos. 114 (D2), D02309.

Andersson, A., Deng, J., Du, K., Zheng, M., Yan, C., Sköld, M., Gustafsson, Ö., 2015. Regionally-varying combustion sources of the January 2013 severe haze events over Eastern China. Environ. Sci. Technol. 49 (4), 2038–2043.

Boylan, J.W., Russell, A.G., 2006. PM and light extinction model performance metrics, goals, and criteria for three-dimensional air quality models. Atmos. Environ. 40 (26), 4946–4959.

Cao, J.-J., Wang, Q.-Y., Chow, J.C., Watson, J.G., Tie, X.-X., Shen, Z.-X., Wang, P., An, Z.-S., 2012. Impacts of aerosol compositions on visibility impairment in Xi'an, China. Atmos. Environ. 59 (0), 559–566.

Castro, L.M., Pio, C.A., Harrison, R.M., Smith, D.J.T., 1999. Carbonaceous aerosol in urban and rural European atmospheres: estimation of secondary organic carbon concentrations. Atmos. Environ. 33 (17), 2771–2781.

Chan, C.K., Yao, X., 2008. Air pollution in mega cities in China. Atmos. Environ. 42 (1), 1–42.

Choi, Y.J., Fernando, H.J.S., 2008. Implementation of a windblown dust parameterization into MODELS-3/CMAQ: application to episodic PM events in the US/Mexico border. Atmos. Environ. 42 (24), 6039–6046.

Cohan, D.S., Hakami, A., Hu, Y.T., Russell, A.G., 2005. Nonlinear response of ozone to emissions: source apportionment and sensitivity analysis. Environ. Sci. Technol. 39 (17), 6739–6748.

Dunker, A.M., Yarwood, G., Ortmann, J.P., Wilson, G.M., 2002. Comparison of source apportionment and source sensitivity of ozone in a three-dimensional air quality model. Environ. Sci. Technol. 36 (13), 2953–2964.

Dzepina, K., Volkamer, R.M., Madronich, S., Tulet, P., Ulbrich, I.M., Zhang, Q., Cappa, C.D., Ziemann, P.J., Jimenez, J.L., 2009. Evaluation of recently-proposed secondary organic aerosol models for a case study in Mexico City. Atmos. Chem. Phys. 9 (15), 5681–5709.

Fast, J.D., Gustafson, W.I., Easter, R.C., Zaveri, R.A., Barnard, J.C., Chapman, E.G., Grell, G.A., Peckham, S.E., 2006. Evolution of ozone, particulates, and aerosol direct radiative forcing in the vicinity of Houston using a fully coupled meteorology-chemistry-aerosol model. J. Geophys. Res.-Atmos. 111 (D21).

Guo, S., Hu, M., Guo, Q., Zhang, X., Zheng, M., Zheng, J., Chang, C.-C., Schauer, J.J., Zhang, R., 2012. Primary sources and secondary formation of organic aerosols in Beijing, China. Environ. Sci. Technol. 46 (18), 9846–9853.

He, L.-Y., Huang, X.-F., Xue, L., Hu, M., Lin, Y., Zheng, J., Zhang, R., Zhang, Y.-H., 2011. Submicron aerosol analysis and organic source apportionment in an urban atmosphere in Pearl River Delta of China using high-resolution aerosol mass spectrometry. J. Geophys. Res. Atmos. 116 (D12), D12304.

Hu, J., Wang, Y., Ying, Q., Zhang, H., 2014a. Spatial and temporal variability of PM2.5 and PM10 over the North China Plain and the Yangtze River Delta, China. Atmos. Environ. 95 (0), 598–609.

Hu, J., Ying, Q., Wang, Y., Zhang, H., 2015. Characterizing multi-pollutant air pollution in China: comparison of three air quality indices. Environ. Int. 84, 17–25 (submitted for publication).

Hu, J., Zhang, H., Chen, S.-H., Wiedinmyer, C., Vandenberghe, F., Ying, Q., Kleeman, M.J., 2014b. Predicting primary PM2.5 and PM0.1 trace composition for epidemiological studies in California. Environ. Sci. Technol. 48 (9), 4971–4979.

Kleeman, M.J., Cass, G.R., 2001. A 3D Eulerian source-oriented model for an externally mixed aerosol. Environ. Sci. Technol. 35 (24), 4834–4848.

Kleeman, M.J., Ying, Q., Lu, J., Mysliwiec, M.J., Griffin, R.J., Chen, J.J., Clegg, S., 2007. Source apportionment of secondary organic aerosol during a severe photochemical smog episode. Atmos. Environ. 41 (3), 576–591.

Kurokawa, J., Ohara, T., Morikawa, T., Hanayama, S., Janssens-Maenhout, G., Fukui, T., Kawashima, K., Akimoto, H., 2013. Emissions of air pollutants and greenhouse gases over Asian regions during 2000–2008: Regional Emission inventory in ASia (REAS) version 2. Atmos. Chem. Phys. 13 (21), 11019–11058.

Lei, Y., Zhang, Q., Nielsen, C., He, K., 2011. An inventory of primary air pollutants and CO_2 emissions from cement production in China, 1990–2020. Atmos. Environ. 45 (1), 147–154.

Li, M., Zhang, Q., Streets, D.G., He, K.B., Cheng, Y.F., Emmons, L.K., Huo, H., Kang, S.C., Lu, Z., Shao, M., Su, H., Yu, X., Zhang, Y., 2014. Mapping Asian anthropogenic emissions of non-methane volatile organic compounds to multiple chemical mechanisms. Atmos. Chem. Phys. 14 (11), 5617–5638.

Lin, P., Hu, M., Deng, Z., Slanina, J., Han, S., Kondo, Y., Takegawa, N., Miyazaki, Y., Zhao, Y., Sugimoto, N., 2009. Seasonal and diurnal variations of organic carbon in PM2.5 in Beijing and the estimation of secondary organic carbon. J. Geophys. Res. Atmos. 114.

Menon, S., Unger, N., Koch, D., Francis, J., Garrett, T., Sednev, I., Shindell, D., Streets, D., 2008. Aerosol climate effects and air quality impacts from 1980 to 2030. Environ. Res. Lett. 3 (2), 024004.

Misenis, C., Zhang, Y., 2010. An examination of sensitivity of WRF/Chem predictions to physical parameterizations, horizontal grid spacing, and nesting options. Atmos. Res. 97 (3), 315–334.

Poschl, U., 2005. Atmospheric aerosols: composition, transformation, climate and health effects. Angew. Chemie-Int. Ed. 44 (46), 7520–7540.

Pui, D.Y.H., Chen, S.-C., Zuo, Z., 2014. PM2.5 in China: measurements, sources, visibility and health effects, and mitigation. Particuology 13 (0), 1–26.

Shaw, W.J., Allwine, K.J., Fritz, B.G., Rutz, F.C., Rishel, J.P., Chapman, E.G., 2008. Evaluation of the wind erosion module in DUSTRAN. Atmos. Environ. 42 (8), 1907–1921.

Streets, D.G., Bond, T.C., Carmichael, G.R., Fernandes, S.D., Fu, Q., He, D., Klimont, Z., Nelson, S.M., Tsai, N.Y., Wang, M.Q., Woo, J.H., Yarber, K.F., 2003. An inventory of gaseous and primary aerosol emissions in Asia in the year 2000. J. Geophys. Res.-Atmos. 108 (D21).

Sun, Y., Jiang, Q., Wang, Z., Fu, P., Li, J., Yang, T., Yin, Y., 2014. Investigation of the sources and evolution processes of severe haze pollution in Beijing in January 2013. J. Geophys. Res. Atmos. 119 (7), 2014JD021641.

Tao, J., Gao, J., Zhang, L., Zhang, R., Che, H., Zhang, Z., Lin, Z., Jing, J., Cao, J., Hsu, S.C., 2014. PM2.5 pollution in a megacity of southwest China: source apportionment and implication. Atmos. Chem. Phys. Discuss. 14 (4), 5147–5196.

Wang, D., Hu, J., Xu, Y., Lv, D., Xie, X., Kleeman, M., Xing, J., Zhang, H., Ying, Q., 2014a. Source contributions to primary and secondary inorganic particulate matter

during a severe wintertime PM2.5 pollution episode in Xi'an, China. Atmos. Environ. 97 (0), 182–194.
Wang, H., Tian, M., Li, X., Chang, Q., Cao, J., Yang, F., Ma, Y., He, K., 2015. Chemical composition and light extinction contribution of PM2.5 in urban Beijing for a 1-year period. Aerosol Air Qual. Res. http://dx.doi.org/10.4209/aaqr.2015.04.0257 (in press).
Wang, L.T., Wei, Z., Yang, J., Zhang, Y., Zhang, F.F., Su, J., Meng, C.C., Zhang, Q., 2013. The 2013 severe haze over the southern Hebei, China: model evaluation, source apportionment, and policy implications. Atmos. Chem. Phys. Discuss. 13 (11), 28395–28451.
Wang, R., Tao, S., Wang, W., Liu, J., Shen, H., Shen, G., Wang, B., Liu, X., Li, W., Huang, Y., Zhang, Y., Lu, Y., Chen, H., Chen, Y., Wang, C., Zhu, D., Wang, X., Li, B., Liu, W., Ma, J., 2012a. Black Carbon Emissions in China from 1949 to 2050. Environ. Sci. Technol 46, 7595–7603.
Wang, S.W., Zhang, Q., Streets, D.G., He, K.B., Martin, R.V., Lamsal, L.N., Chen, D., Lei, Y., Lu, Z., 2012b. Growth in NOx emissions from power plants in China: bottom-up estimates and satellite observations. Atmos. Chem. Phys 12 (10), 4429–4447.
Wang, Y., Ying, Q., Hu, J., Zhang, H., 2014b. Spatial and temporal variations of six criteria air pollutants in 31 provincial capital cities in China during 2013–2014. Environ. Int. 73 (0), 413–422.
Wiedinmyer, C., Akagi, S.K., Yokelson, R.J., Emmons, L.K., Al-Saadi, J.A., Orlando, J.J., Soja, A.J., 2011. The Fire INventory from NCAR (FINN): a high resolution global model to estimate the emissions from open burning. Geosci. Model Dev. 4, 625–641.
Ying, Q., Lu, J., Kaduwela, A., Kleeman, M., 2008. Modeling air quality during the California REGIONAL PM10/PM2.5 Air Quality Study (CPRAQS) using the UCD/CIT Source Oriented Air Quality Model - Part II. Regional source apportionment of primary airborne particulate matter. Atmos. Environ. 42 (39), 8967–8978.
Ying, Q., Wu, L., Zhang, H., 2014. Local and inter-regional contributions to PM2.5 nitrate and sulfate in China. Atmos. Environ. 94 (0), 582–592.
Zhang, H., Chen, G., Hu, J., Chen, S.-H., Wiedinmyer, C., Kleeman, M., Ying, Q., 2014a. Evaluation of a seven-year air quality simulation using the Weather Research and Forecasting (WRF)/Community Multiscale Air Quality (CMAQ) models in the eastern United States. Sci. Total Environ. 473–474 (0), 275–285.
Zhang, H., DeNero, S.P., Joe, D.K., Lee, H.H., Chen, S.H., Michalakes, J., Kleeman, M.J., 2014b. Development of a source oriented version of the WRF/Chem model and its application to the California regional PM10/PM2.5 air quality study. Atmos. Chem. Phys. 14 (1), 485–503.
Zhang, H., Li, J., Ying, Q., Yu, J.Z., Wu, D., Cheng, Y., He, K., Jiang, J., 2012. Source apportionment of PM2.5 nitrate and sulfate in China using a source-oriented chemical transport model. Atmos. Environ. 62 (0), 228–242.
Zhang, H., Wang, Y., Hu, J., Ying, Q., Hu, X.-M., 2015. Relationships between meteorological parameters and criteria air pollutants in three megacities in China. Environ. Res. 140 (0), 242–254.
Zhang, H., Ying, Q., 2011. Contributions of local and regional sources of NOx to ozone concentrations in Southeast Texas. Atmos. Environ. 45 (17), 2877–2887.
Zhang, Q., Streets, D.G., Carmichael, G.R., He, K.B., Huo, H., Kannari, A., Klimont, Z., Park, I.S., Reddy, S., Fu, J.S., Chen, D., Duan, L., Lei, Y., Wang, L.T., Yao, Z.L., 2009. Asian emissions in 2006 for the NASA INTEX-B mission. Atmos. Chem. Phys. 9 (14), 5131–5153.
Zhang, R., Jing, J., Tao, J., Hsu, S.C., Wang, G., Cao, J., Lee, C.S.L., Zhu, L., Chen, Z., Zhao, Y., Shen, Z., 2013. Chemical characterization and source apportionment of PM2.5 in Beijing: seasonal perspective. Atmos. Chem. Phys. 13 (14), 7053–7074.
Zhang, R., Khalizov, A.F., Pagels, J., Zhang, D., Xue, H., McMurry, P.H., 2008. Variability in morphology, hygroscopicity, and optical properties of soot aerosols during atmospheric processing. Proc. Natl. Acad. Sci. U. S. A. 105, 10291–10296.
Zhao, X.J., Zhao, P.S., Xu, J., Meng, W., Pu, W.W., Dong, F., He, D., Shi, Q.F., 2013. Analysis of a winter regional haze event and its formation mechanism in the North China Plain. Atmos. Chem. Phys. 13 (11), 5685–5696.
Zheng, B., Huo, H., Zhang, Q., Yao, Z.L., Wang, X.T., Yang, X.F., Liu, H., He, K.B., 2014. High-resolution mapping of vehicle emissions in China in 2008. Atmos. Chem. Phys. 14 (18), 9787–9805.